JOURNAL OF MATERIALS SCIENCE 27 (1992) 6490–6494

Effect of sinter duration on the mechanical properties of a tungsten alloy

R. G. O'DONNELL, S. J. ALKEMADE, R. L. WOODWARD
Materials Research Laboratory, PO Box 50, Ascot Vale 3032, Victoria, Australia

The effect of sinter duration on the tensile strength and ductility in tension of a 95%W–3.5%Ni–1.5%Fe alloy was shown to be negligible. The alloy showed a broad ductile to brittle transition as the testing temperature was reduced below 100 °C, and this was also unaffected by the sinter duration. Despite the negligible change in mechanical properties with sinter duration, the fracture mode changed with an increased proportion of transgranular tungsten grain fracture at the expense of tungsten–tungsten interface fracture, at the longer sintering times. Quantitative metallography showed that grain size increases and tungsten–tungsten spheroid interface area decreased with increasing sintering time. The mechanical property and fracture morphology observations have been interpreted in terms of these microstructural changes.

1. Introduction

Tungsten–nickel–iron alloys are manufactured by liquid-phase sintering green compacts of the elemental powders at temperatures in the range 1450–1500 °C, at which a nickel–iron–tungsten liquidus is in equilibrium with solid tungsten. Tungsten spheroid growth occurs by a process called Ostwald ripening, during which smaller particles dissolve with re-precipitation on to the larger tungsten particles, the driving force being the reduction in surface energy achieved [1]. Spheroid coalescence, where particles of similar crystallographic orientation come into contact and subsequently continue to grow as one, also contributes to grain growth during sintering [1, 2]. The resulting alloy consists of a semi-contiguous network of tungsten spheroids surrounded by a ductile matrix phase.

The mechanical properties of these alloys, especially their strength and ductility, are very sensitive to manufacturing parameters such as sintering conditions and initial powder purity [3]. This has led to a number of studies which attempted to identify the causes of the observed widespread variation in mechanical properties and which proposed manufacturing techniques both to minimize the property variations and to maximize alloy strength and ductility [3–6]. Of these, the sinter duration is important not only because of its effect on mechanical properties but also because it influences the cost of processing these alloys. Consequently, it is desirable to keep sintering time to a minimum whilst still ensuring suitable mechanical properties are retained.

The present work addressed the effect of sinter duration and test temperature on the mechanical properties of a 95%W–3.5%Ni–1.5%Fe tungsten alloy. The manufacture of this alloy using a 2 h sintering time has been discussed in detail [7] and previous studies have characterized the effects of strain rate [8, 9] and test temperature [10] on its mechanical behaviour.

2. Experimental procedure

The liquid-phase sintered tungsten alloy blanks, were of nominal composition (wt%) 95 W, 3.5 Ni and 1.5 Fe. The blanks had been sintered at 1500 °C in a hydrogen atmosphere for times varying from 0.5–3 h in 0.5 h increments. The blanks were all subsequently vacuum annealed for 3 h at 1100 °C.

The blanks were machined into tensile test specimens of diameter 4.1 mm and gauge length 20 mm and tensile tests were conducted in a screw-driven machine at an average strain rate of $1.5 \times 10^{-4} s^{-1}$. Test temperatures ranged from -100 to 100 °C to enable the effect of sintering duration on the ductile to brittle transition to be examined. Data are presented on ultimate tensile strength (UTS), fracture strain and reduction of area; the latter two may be used as a measure of alloy ductility.

Sections of fracture surfaces were examined by optical metallography and the fracture surface by scanning electron microscopy. To assist in interpretation of the fracture data, quantitative metallographic methods were used to determine tungsten particle size, tungsten particle to particle contact area and tungsten particle contiguity, as a function of sintering time.

3. Results

Data from the ambient temperature tensile tests are tabulated in Table I along with the quantitative metallographic data. Despite a significant increase in grain size and reduction in tungsten to tungsten particle contact area with increased sintering time, there is little variation in the mean values of UTS, reduction of

0022–2461

TABLE I Effect of sinter duration of grain size, particle to particle contact area, contiguity and ambient temperature mechanical properties

Sintering time (h)	Tungsten spheroid size (μm)	Tungsten to tungsten spheroid contact area per unit volume (mm^{-1})	Tungsten Particle contiguity	UTS (MPa)	Elongation (%)	Reduction of area (%)
0.5	27.9	31.1	0.44	915	22	19
1.0	30.5	22.5	0.34	910	27	24
1.5	36.6	19.4	0.35	905	23	19
2.0	35.6	19.3	0.34	905	24	20
2.5	42.2	15.4	0.32	900	27	22
3.0	40.9	14.8	0.30	905	25	20

area and elongation. The effect of sintering time on grain size is illustrated by the typical sections of samples sintered for 0.5 and 3 h in Fig. 1a and b, respectively.

Tensile test data are plotted as a function of test temperature in Fig. 2, which shows no effect of sinter duration, within the scatter of data, on either strength or ductility, except that a small number of low-ductility results are observed for the shorter sintering times. Those specimens showing low ductility also exhibited anomalously high percentages of intergranular failure. That such anomalies were not observed at longer sintering times indicates that interface strength increases with sintering time to a consistently acceptable value after 1 h sinter duration. Whilst Table I shows a large drop in tungsten particle contiguity between 0.5 and 1.0 h sintering, the fractography indicated that all interfaces were involved in the more brittle failures, not just tungsten–tungsten interfaces. The general trend in Fig. 2 is for strength to decrease and ductility to increase as testing temperature increases.

Scanning electron microscopy showed fracture was largely intergranular, but with some cleavage, at the shorter sinter durations, and of the order of 50% intergranular and 50% cleavage at the longer durations, as shown in the typical fracture surfaces in Fig. 3. The high elongations at all sintering times and the mixed nature of the fracture type indicates that the strength of the interfaces is of similar magnitude to the strength of the tungsten grains. An increase in the percentage of transgranular fracture also accompanied an increase in test temperature. A section through a specimen tested at 100 °C, Fig. 4, shows that tungsten spheroid cleavage plays a large role in fracture of this alloy even at elevated temperatures. Earlier work on this alloy [10] shows almost 100% cleavage at test temperatures of 300 °C, contrary to observations on other tungsten alloys [11] which note a decrease in transgranular fracture accompanying an increase in test temperature.

4. Discussion

Several authors [5, 11] have identified four principal modes of fracture in sintered tungsten alloys as illustrated in Fig. 5: (i) matrix–matrix failure, (ii) matrix–tungsten spheroid interfacial separation, (iii) tungsten spheroid–tungsten spheroid intergranular failure, and (iv) tungsten spheroid fracture. Of these fracture modes, that most commonly reported as requiring the least energy of fracture is intergranular failure along the grain boundary between adjoining tungsten spheroids [3–5, 11]. During tensile deformation the intergranular failure sites on the surface of the specimen act

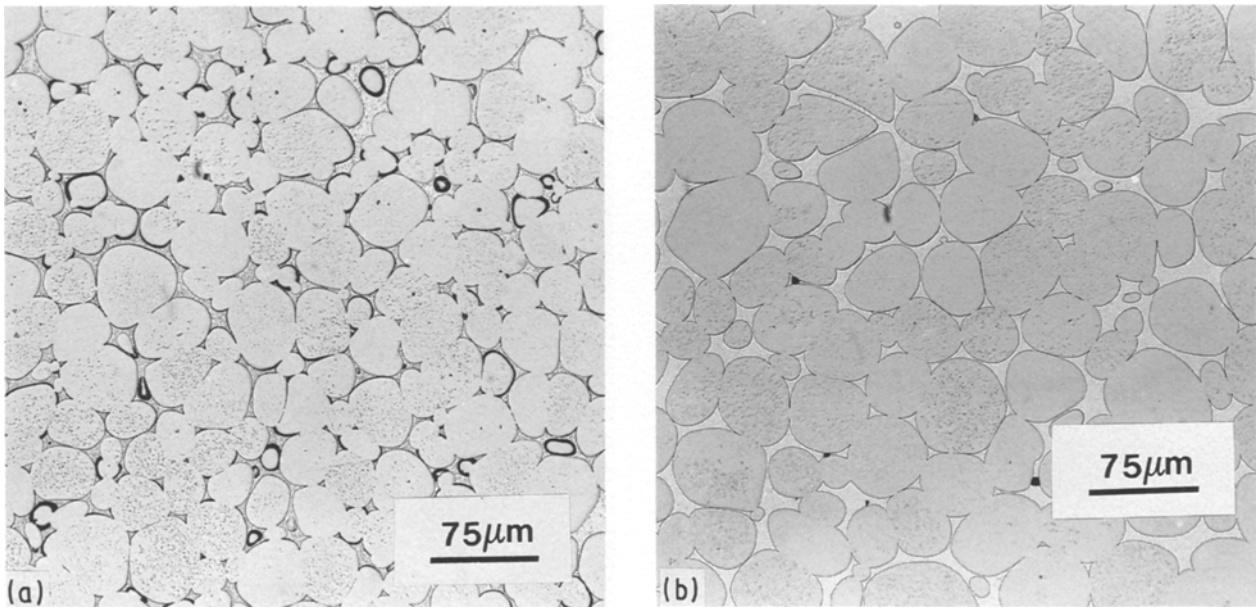

Figure 1 Microstructures of a tungsten alloy sintered for (a) 0.5 h and (b) 3.0 h, showing the increase in tungsten spheroid size with sinter duration.

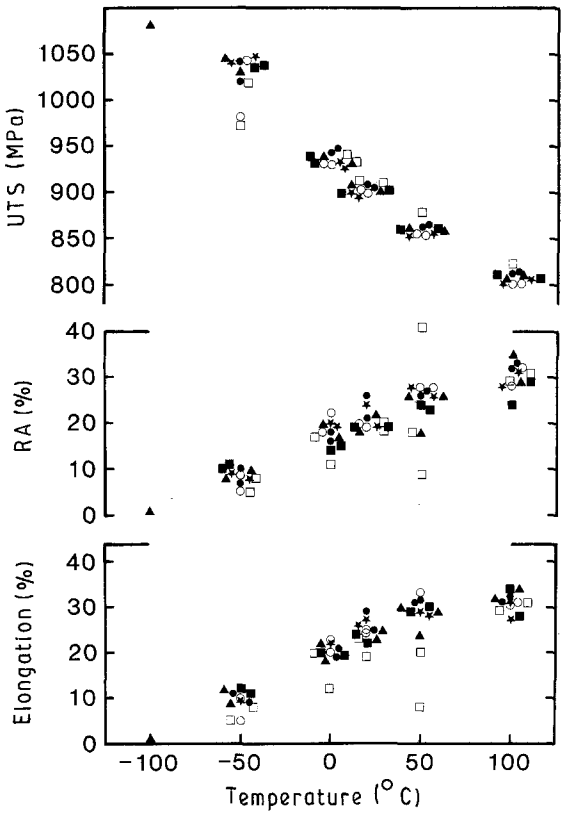

Figure 2 Plots of UTS, elongation and reduction of area as a function of test temperature for all the sintering times: (□) 0.5 h, (●) 1.0 h, (■) 1.5 h, (▲) 2.0 h, (★) 2.5 h, (○) 3.0 h.

as notches [4, 6] and fractures initiate from these sites [5], as illustrated in Fig. 4 for the present material. However, at the time of failure, crack nuclei are also evident at many internal sites. The propagation of cracks initiated at the surface may be impeded, or indeed arrested, by the surrounding matrix material. However, when a crack is able to continue propagating it will follow the path requiring the least fracture energy.

The occurrence of increased spheroid fracture is often associated with increased alloy strength [1, 5, 12] although ambient temperature tensile tests in the present instance indicate no consistent trend in either alloy strength (UTS) or ductility with sinter duration (Table I) despite such a variation in fracture mode. Whilst statistical variations inherent in these tensile tests may obscure any minor dependence of mechanical properties on sinter duration, similar data determined over a range of test temperatures also show no conclusive evidence for such a dependence, Fig. 2. The observation of no significant effect of sinter duration on ductility is supported by the results of Rabin and German [4] for a twenty-fold increase in sintering time with a similar alloy; however, this same work shows a decrease in strength with sinter duration. These authors also considered spheroid growth due to increased sintering temperatures (a further manufacturing variable which can produce equivalent changes in the spheroid size distribution [1]) and noting a similar trend, attribute the drop in strength to an increase in the size of tungsten–tungsten intergranular boundary areas, and hence in fracture sites, which accompanies an increase in spheroid size. A similar conclusion was reached earlier by Eisenmann and German [3]. This explanation, however, requires that the crack path become increasingly intergranular at the expense of transgranular fracture as the spheroid size increases, contrary to the present observations.

Simple geometrical arguments show that, for a constant volume fraction of the tungsten spheroid phase, the total spheroid surface area per unit volume is inversely proportional to the particle diameter. Quantitative stereological methods demonstrate, with the present alloy, that the total particle to particle contact area reduces substantially with increase in spheroid size, Table I. The data of Table I are indicative of approximately 30% tungsten spheroid surface area, on average, being taken up by tungsten–tungsten

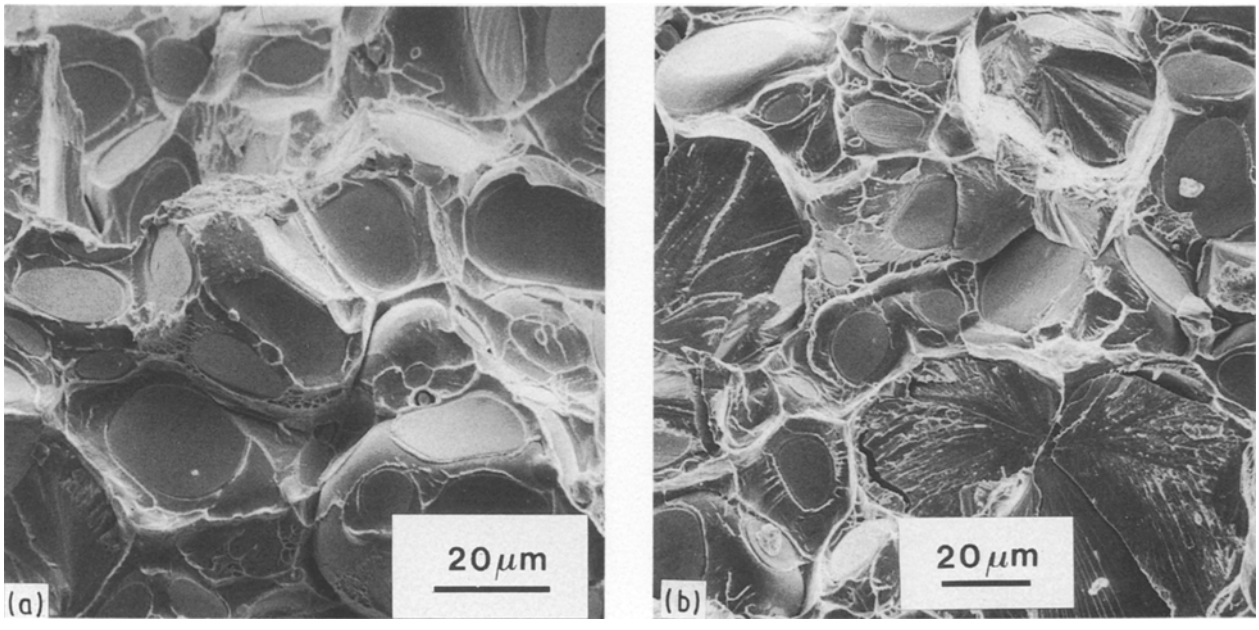

Figure 3 Scanning electron micrographs of ambient temperature tensile fracture surfaces of samples sintered for (a) 0.5 h and (b) 2.5 h.

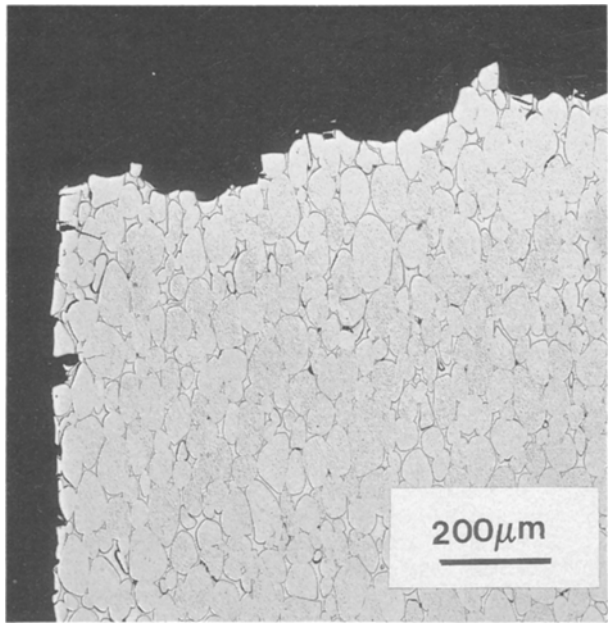

Figure 4 Section through the fracture surface (top of figure) of a specimen sintered for 3 h and fractured in tension at 100 °C. Cracks initiating from the specimen's cylindrical surface are evident to the left of the figure.

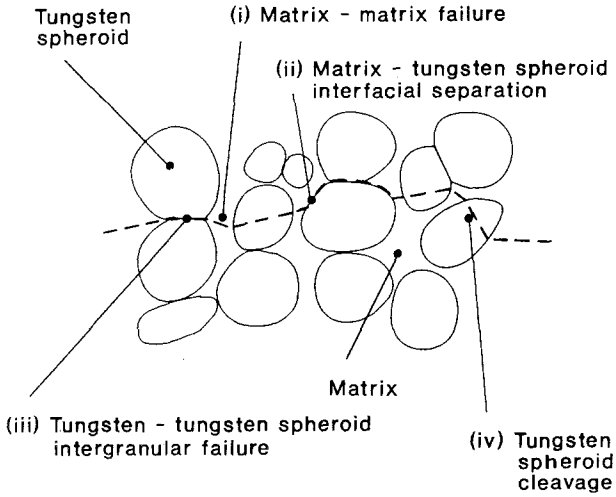

Figure 5 Schematic illustration of the principal fracture modes in tungsten alloys.

contacts, except in the case of the 0.5 h sinter where it is substantially larger, with total area reducing substantially as sintering time increases. These observations conform with the geometry of packing of spheres, so that earlier explanations based on increased particle to particle contact area with increased particle diameter are not acceptable.

The observation that sintering time does not affect ductility or strength in the present alloy, despite a change in fracture mode, may be explained as follows. The observation of a mixed fracture mode indicates that there is not a big difference in toughness between the intergranular and transgranular mechanisms for this present alloy. Examination of fracture surfaces, Fig. 3, shows that the intergranular failures are dominated by the tungsten–tungsten contact region. It is suggested that as particle size increases the availability of tungsten–tungsten contact area as a fracture path decreases (Table I) and the crack deviation required to maintain that path increases because of the increased spheroid size. As a consequence, the fracture mechanism switches to the next weakest mode, which may be tungsten particle cleavage. Because of the small difference in toughness between these mechanisms as noted above, this change does not result in an increase in macroscopically observed toughness, within the scatter of data, for the present alloy. The explanation requires that the tungsten particle interfacial boundaries be strong in the present alloy.

There are differences in microstructure between the present alloy and that of nominally identical composition investigated by German and co-workers [3, 4, 11]. The data of Rabin and German [4] suggests a mean tungsten spheroid size of 21 μm following 0.5 h sinter duration, increasing to 28 μm after 2 h. This is compared with mean diameters of 28 and 36 μm, respectively, for the present alloy sintered for the same times. The higher sintering temperature for the present alloy compared with that for Rabin and German's alloy, i.e. 1500 °C compared to 1480 °C, does not account for the significantly larger spheroid diameters exhibited in the present case [4]. Clearly the sintering kinetics of these alloys differ and this may result from different initial elemental powder sizes, purity, or powder mixing effectiveness.

The larger spheroid diameter exhibited by the present alloy should contribute to a reduction in alloy strength due to an increase in intergranular fracture, according to the arguments presented by German and co-workers [3–5], although, as noted earlier, this was not the case. The reason for this discrepancy appears to be related to the difference in the failure mechanism of the two alloys. The occurrence of intergranular fracture between the spheroids away from the primary fracture surface is rare in the present alloy even at the failure strain, see Fig. 4, while the alloy of Rabin and German already exhibits extensive intergranular fracture at 13.7% strain [4]. Failure in that latter alloy occurs through the linking of these intergranular cracks, while this is clearly not the case for the present alloy, Fig. 4. This difference may be attributed to a higher tungsten interfacial boundary strength in the present alloy.

An explanation for reduced ductility and increased intergranular fracture with increased particle size, as shown by Rabin and German [4], may come from the effects of impurities on grain-boundary fracture. If intergranular fracture is affected by minor impurity elements, then the reduced total boundary area consequent on an increased grain size will lead to greater impurity concentration per unit area and one may go from a mixed failure mode where the boundary-weakening effect is sparse at the small grain size, to a totally intergranular mode where the weakening effect covers all boundaries at the larger grain size. Even if intergranular fracture is already dominant at the smaller grain size, the degree of weakening should increase with increased impurity concentration per unit area as the grain size increases, thus leading to reduced

strength without an observed change in fracture mechanism. This explanation is consistent with the extensive intergranular fracture noted at moderate strains in the alloy of Rabin and German [4], as noted above.

5. Conclusion

An increased sinter duration is shown to increase the amount of transgranular tungsten fracture at the expense of intergranular fracture in tensile fracture of a 95% W, 3.5% Ni, 1.5% Fe alloy. Despite the change in fracture mode, the strength and toughness of the tungsten alloy are not affected by the increase in sinter duration. Microstructural examination shows that grain size increases markedly between the shortest, 0.5 h, and largest, 3 h, sinter durations and there is a concomitant large reduction in both total tungsten boundary area and tungsten to tungsten grain contact area. The results are explained in terms of a relatively small difference in strength of the tungsten cleavage and tungsten–tungsten grain interface fracture paths for the present alloy, and the effect of microstructural changes on the availability of interface fracture area. The alloy exhibits a broad ductile to brittle failure transition as the test temperature is reduced below 100 °C, and this is accompanied by a decrease in the amount of transgranular tungsten fracture and an increase in intergranular fracture as the temperature decreases. Sinter duration has no discernible effect on the ductile to brittle transition. The mechanical behaviour of this alloy is clearly different to that observed by other researchers in nominally identical alloys, and this is attributable to the greater strength of intergranular boundaries in the present alloy.

Acknowledgements

The authors acknowledge the technical assistance provided by Alban Cole, Patrick McCarthy and Richard Muscat.

References

1. E. G. ZUKAS and H. SHEINBERG, *Powder Technol.* **13** (1976) 85.
2. J. B. POSTHILL, M. C. HOGWOOD and D. V. EDMONDS, *Powder Metall.* **29** (1986) 45.
3. M. R. EISENMANN and R. M. GERMAN, *Int. J. Refract. Hard Metals* **3** (1984) 86.
4. B. H. RABIN and R. M. GERMAN, *Met. Trans.* **19A** (1988) 1523.
5. B. H. RABIN, A. BOSE and R. M. GERMAN, in "Microstructural Science", Vol. 15, edited by M. E. Blum, P. M. French, R. M. Middleton and G. F. Vander Voort (Elsevier, New York, 1986) pp 285–99.
6. W. E. GURWELL, in "Annual Powder Metallurgy Conference and Exhibition", Boston MA (Metal Powder Industries Federation, 1986) pp. 1–15.
7. R. L. WOODWARD, J. M. YELLUP and M. E. de MORTON, *Met. Forum* **6** (1983) 175.
8. R. L. WOODWARD, N. J. BALDWIN, I. BURCH and B. J. BAXTER, *Metall. Trans.* **16A** (1985) 2031.
9. S. J. CIMPOERU and R. L. WOODWARD, *J. Mater. Sci. Lett.* **9** (1990) 187.
10. R. G. O'DONNELL and R. L. WOODWARD, *Met. Trans.* **21A** (1990) 744.
11. R. M. GERMAN, J. E. HANAFEE and S. L. DIGIALLONARDO, *ibid.* **15A** (1984) 121.

Received 3 September 1991
and accepted 17 February 1992